Energy Technology
Generation, Conversion, Storage, Distribution
www.entechnol.de

X-Ray-Computed Radiography and Tomography Study of Electrolyte Invasion and Distribution inside Pristine and Heat-Treated Carbon Felts for Redox Flow Batteries

Marcus Gebhard, Maike Schnucklake, André Hilger, Maximilian Röhe, Markus Osenberg, Ulrike Krewer, Ingo Manke, and Christina Roth*

Porous carbon felts (CFs) are widely used electrode materials for vanadium redox flow batteries (VRFBs). These materials differ in their precursor material, thickness, or graphitization degree and demonstrate broad differences in electrochemical performance. Prior to operation, an activation step, such as acid or heat treatment (HT), is commonly performed to improve their performance. A thermal treatment in air functionalizes the surface of the electrode and improves reaction kinetics as well as the wettability of the electrode. Herein, pristine and heat-treated CFs are compared regarding their electrolyte wetting behavior for the use in VRFB. Contact angle (CA) measurements are conducted ex situ to investigate the effect of the HT. Furthermore, the porous CFs are examined in situ with an in-house-built flow cell regarding their invasion behavior with different types of electrolytes by X-ray radiography. Additionally, the distribution of the electrolyte inside the felts is investigated by X-ray tomography. The results demonstrate the effect of the HT and choice of electrolyte on the wetting behavior and electrolyte distribution.

1. Introduction

To ensure a steady and stable supply of power, large-scale energy systems are needed to cope with the increasing implementation of only intermittently available renewable energy to the grid. Vanadium redox flow batteries (VRFBs) are a promising technology, where the energy is stored in the form of aqueous electrolyte solutions.[1] With this technique, dissolved vanadium ions in four different oxidation states serve as electrolytes for the positive (V^{4+}/V^{5+}) and the negative (V^{2+}/V^{3+}) half-cell reaction. They are pumped through porous electrode materials in a flow through geometry, whereby the compressed electrodes act as heterogeneous reaction surfaces.[2]

The most prominent electrode materials are commercially available polyacrylonitrile- or rayon-based carbon felts (CFs), which after graphitization exhibit good electrical conductivity combined with a comparatively low cost and stability in acidic environment.[3] However, they show poor wettability and low activity toward the redox reactions of vanadium. Several approaches have been reported in the literature to enhance the electrochemical activity of the felts, for instance, decorating the surface with different metals or metal oxides[4] as well as enhancing the surface area of the felts to increase contact between electrode and electrolyte.[5] But the most commonly used strategy is their oxidation, which can be achieved in a controlled manner either by oxidizing acid or by heat treatment (HT), where the latter is the preferred strategy.[6] To this end, a thermal treatment is applied by heating the

M. Gebhard, Prof. C. Roth
Electrochemical Process Engineering
Universität Bayreuth
Universitätsstraße 30, Bayreuth 95447, Germany

M. Schnucklake
Institute of Chemistry and Biochemistry
Freie Universität Berlin
Takustraße 3, Berlin 14195, Germany
E-mail: maike.schnucklake@fu-berlin.de

The ORCID identification number(s) for the author(s) of this article can be found under https://doi.org/10.1002/ente.201901214.

© 2019 The Authors. Published by WILEY-VCH Verlag GmbH & Co. KGaA, Weinheim. This is an open access article under the terms of the Creative Commons Attribution-NonCommercial-NoDerivs License, which permits use and distribution in any medium, provided the original work is properly cited, the use is non-commercial and no modifications or adaptations are made.

DOI: 10.1002/ente.201901214

Dr. A. Hilger, M. Osenberg, Prof. I. Manke
Institute of Applied Materials
Helmholtz-Zentrum Berlin für Materialien und Energie GmbH
Hahn-Meitner-Platz 1, Berlin 14109, Germany

M. Röhe, Prof. U. Krewer
Institute of Energy and Process Systems Engineering
Technische Universität Braunschweig
Franz-Liszt-Str. 35, Braunschweig 38106, Germany

M. Osenberg
Department of Materials Science and Technology
Technische Universität Berlin
Hardenbergstr. 36, Berlin 10623, Germany

felts for 30 h under air, increasing the temperature to 400 °C. This activation step may improve their wettability, due to an increased amount of oxidized functional groups on the electrode surface. In previous works, it was found that an enhancement of functional groups causes a decrease in the sp^2 content, which is connected with a change in the sp^2/sp^3 ratio of the carbon surface and this proves to be beneficial for the overall performance.[7] So far, details of the mechanism have not been clarified yet and various opinions about the specific requirements needed for an optimal electrode material are discussed in the literature.[7a,8] Accordingly, the actual influence of the improved wetting behavior as well as the general significance of wetting have to be studied by more application-oriented in situ experiments.

For this purpose, X-ray imaging techniques may be a suitable approach as they can trace the invasion and distribution of the V-containing electrolyte within the porous CF electrodes. Such techniques have been widely used,[9] in particular, to investigate the transport paths of water in polymer electrolyte membrane fuel cells.[10] The obtained information is then applied for a rational choice of operation parameters and flow-field geometries. Recently, this method has turned out as a useful tool in understanding the electrode wetting phenomena in redox flow batteries as well. However, only some publications concerning this issue exist so far.[5b] Tariq et al.[11] outlined the electrolyte permeation in dry carbon paper electrodes utilizing time-resolved 3D X-ray tomography. They highlighted a non-uniform progression front, where initially smaller channel-like pores are filled, which serve as favored pathways for the electrolyte. Then, the bigger pores are filled with electrolyte. Also, Banerjee et al.[12] used this technique to compare different carbon electrode materials concerning their internal pore structures and transport properties. They found out that an increased wettability has a strong impact on the imbibition curve, lowering the pressure which is necessary for the electrolyte to invade into the carbon material. Greco et al.[13] examined thermal-oxidized carbon paper electrodes, to show a contrary correlation between the content of surface oxygen groups and the electrochemical active surface area (ECSA), and linked these to the cell performance of the battery. In a very recent publication, Zeis and coworkers[14] analyzed the initial wetting behavior, saturation, and pressure drop of untreated (UT) and heat-treated carbon electrodes. It has been observed that the introduction of functional groups facilitates a thorough wetting, which leads to higher saturation inside the CF and therefore to an increased ECSA. However, the in situ cell which has been used in this study was designed to optimize the radiography conditions and needed therefore significant modifications with respect to size and geometry.

In this work, we want to analyze the influence of the thermal treatment on the wetting behavior of carbon electrodes by two different investigation methods. Measuring contact angles (CAs) is the most frequently used method to examine the wetting behavior of different materials. Those measurements are facile to conduct, but issues exist with respect to their correct interpretation and adaptation to real conditions. That is why we complemented these qualitative data, by in situ X-ray radiography and tomography in an application-oriented in situ cell to follow the invasion behavior and electrolyte distribution inside CFs under realistic conditions. We demonstrate the effect of the thermal treatment on the wetting behavior for different electrolytes using X-ray imaging.

2. Experimental Section

Unless otherwise stated, all chemicals were used as received without further purification.

2.1. Electrode Materials and Preparation

Two commercial CF electrodes from SIGRACELL battery electrodes (SGL Carbon SE, Wiesbaden, Germany) were used in this study. CF GFD 4.6 and GFA 6 have comparable properties but differ in the precursor material. The pristine felts were used as received and named with the suffix "UT" (for untreated). The HT of the CFs was executed according to a previously described procedure.[6a] The carbon electrodes were placed in a tube furnace (Carbolite Gero GmbH & Co. KG, Neuhausen, Germany) under air atmosphere and heated at 5 K min^{-1} up to 400 °C. The temperature was held for 10 or 30 h, giving the electrodes the respective suffix "HT 10/HT 30." After thermal treatment, almost no change in mass was observed. For use in further characterization and treatment, all felts were cut into a rectangular shape of 2 × 3 cm.

2.2. CA Measurements

The ex situ surface wettability of the CF electrodes was measured by the analysis of CAs (drop-shape analysis). The static CA was measured for pristine and heat-treated CFs using a drop-shape analyzer DSA 30 (KRÜSS GmbH, Hamburg, Germany) at room temperature (23.0 ± 0.5 °C) in a closed chamber at ambient pressure.

GFD 4.6 UT and the GFD 4.6 HT 30 electrodes were tested 15 times each with 10 µL deionized water (Merck Millipore, Burlington, MA, USA), 2 M sulfuric acid (95% purity, Roth, Germany; Merck Millipore, Burlington, MA, USA), and commercially available VRFB electrolyte, 0.8 M V^{3+}/ 0.8 M V^{4+}, in 2 M H_2SO_4 and 0.05 M H_3PO_4 aqueous solution (GfE mbH, Nürnberg, Germany). The droplets were placed on the electrode with an Eppendorf pipette (Eppendorf AG, Hamburg, Germany). For CAs, computing the tangential method "Tangent–1" has been chosen, base line and focus have been set manually. The given angle is the average of the individual measured values of the left and the right side of the droplet.

2.3. In Situ Cell Design

In situ imaging of the electrodes was performed using an in-house-built flow cell setup. The design of the flow cell was derived from commercially available test cells and was specially modified with respect to the imaging properties. For enabling the imaging of the electrodes with X-ray radiation, the cell was constructed, aiming at minimal impairment by radiation-absorbing materials in the beam path direction. Polyether ether keton (PEEK) endplates formed the general cell geometry, provided high material strength, and were stable against chemical and

© 2019 The Authors. Published by WILEY-VCH Verlag GmbH & Co. KGaA, Weinheim

radiation corrosion.[15] Viton gaskets sealed all components of the cell. Polycarbonate (PC) spacers were manufactured to form the flow field in a flow through geometry with an active electrode area of 2 × 3 cm. In addition, the PC spacers were used in various thicknesses to enable a comparable compression of the felt electrodes. In brief, this setup provided a constant compression of the felt electrodes as well as a homogeneous flow of electrolyte in the cell combined with a minimal absorption of radiation by the cell materials. A schematic 3D visualization of the flow cell and the flow plate design is shown in **Figure 1**.

2.4. Micro-CT Measurements

The laboratory X-ray microcomputed tomography setup consisted of a Hamamatsu X-ray tube (L8121-03, tungsten anode, Hamamatsu Photonics K.K., Hamamatsu) and a Hamamatsu flat panel detector (C7942SK-05, Hamamatsu Photonics K.K., Hamamatsu, Japan). The in situ cell was placed between the source and detector on a rotation desk and was connected to a 100 mL reservoir tank (see **Figure 2**). The electrolyte was pumped with a peristaltic pump (Cyclo I, Carl Roth GmbH + Co. KG, Karlsruhe, Germany) in a closed circuit with a pump rate of 5–25 mL min^{-1}. The 6 cm^2 rectangular-shaped felts were compressed to the same ratio by the use of different spacers. For each experiment either deionized water (Merck Millipore, Burlington, MA, USA), 2 M sulfuric acid (Carl Roth GmbH + Co. KG, Karlsruhe, Germany), or a commercially available VRFB electrolyte 0.8 M V^{3+}/ 0.8 M V^{4+} in 2 M H_2SO_4 and 0.05 M H_3PO_4 aqueous solution (GfE mbH, Nürnberg, Germany) was used. It should be noted here that all tests were done on separate, fresh samples to exclude any effect of previous contact with electrolyte. With the radiography setup imaging the whole flow field, a pixel size of 15 µm was obtained. To achieve maximum contrast and the best signal-to-noise ratio, the X-ray tube was operated at 60 kV and at 160 µA. The normalization of the captured images was performed using the imaging software Fiji (v1.5.2).[16] For low-resolution in situ tomography, the same energy and current were used as during the radiography experiments. At 1200 angle steps, three frames with an exposure time of 0.6 s per frame were taken. In addition, 15 dark- and 15 flatfields were captured. The source object distance was 75 mm and the source detector distance was 250 mm, resulting in a pixel size of 15 µm equivalent to the radiography measurements. For higher resolved ex situ tomography, the tube was operated at 40 kV with a current of 250 µA. The exposure time was increased to 5 s per frame and each of the 1500 angle steps was exposed five times. The source object distance was 59 mm and the source detector distance 500 mm, resulting in a pixel size of 5.9 µm. The schematic illustration of the experimental setup is shown in Figure 2.

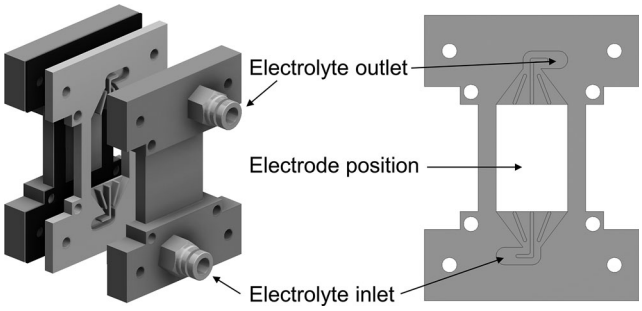

Figure 1. Schematic 3D visualization of the flow cell and the flow plate design.

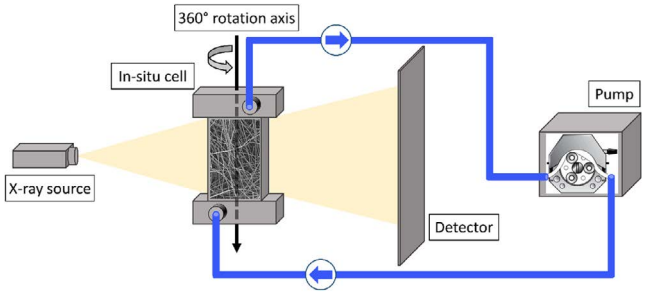

Figure 2. Schematic illustration of the experimental setup including X-ray source, in situ cell, detector, and peristaltic pump.

3. Results and Discussion

In this work, two commonly used pristine CF materials (GFD 4.6/ GFA 6) were heat treated for 10 h and 30 h (HT 10/30), respectively, to investigate and identify the exclusive effect of the HT on the wetting behavior. CA measurements were conducted in an ex situ experiment for the pristine and heat-treated CFs and were exemplary demonstrated for GFD 4.6 in **Figure 3**a–f with each electrolyte.

As shown in the images (Figure 3a–f), each combination of CF and electrolyte exhibits a strong hydrophobic nature. All measurements were conducted multiple times for better statistical analysis, due to the strong deviation experienced during drop-shape analysis. The summarized results in Figure 3g reveal that the contact of an untreated felt with deionized water showed the highest CA with a mean value of around 142°. Sulfuric acid improved the contact and led to a slightly lower CA with a mean value of 137° for the UT sample. When the drop-shape analysis was performed with the commercial VRFB electrolyte, an even lower CA with a mean value of 135° could be observed. This trend implies that the wetting of an untreated CF will be improved when the commercial electrolyte is used. The heat-treated GFD 4.6 CFs showed the same trend as the untreated samples regarding the electrolyte influence but revealed an overall lower CA. The experiment using deionized water showed a decreased hydrophobicity with a lower mean value of 138° compared with 142° for the UT sample. The CA was also measured for the HT sample with sulfuric acid and commercial VRFB electrolyte with an even lower CA of 126–127°. This result supports the generally drawn assumption that the thermal treatment in air will improve the wetting behavior of CFs. Nevertheless, the resulting CAs are still very high and the material must be considered as hydrophobic material.[17]

Thermal oxidation is commonly used to improve the performance of carbon electrodes in VRFB. Also, the resulting enhanced performance is either explained by favorable surface groups,[18] leading to improved kinetics, or by an increased hydrophilicity, therefore an improved wetting behavior and a

© 2019 The Authors. Published by WILEY-VCH Verlag GmbH & Co. KGaA, Weinheim

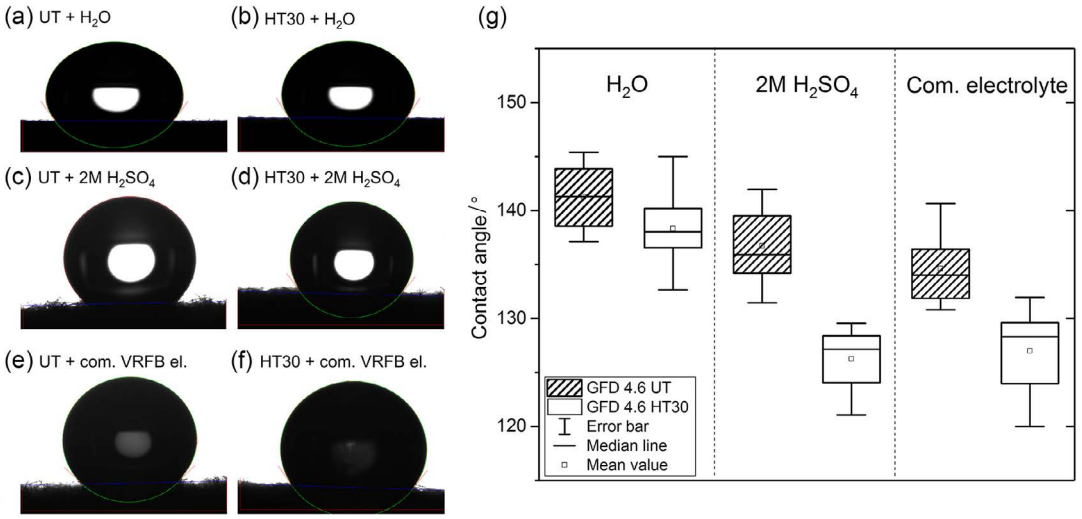

Figure 3. a–f) Photographic images of drop-shape analysis of GFD 4.6 UT/ HT 30 with deionized water, 2 M sulfuric acid, and commercial VRFB electrolyte. g) Graphical representation of drop-shape analysis results.

higher utilization of the electrode. Both attempts of explanations appear valid and would make the electrode favorable for electrochemical reactions.[19] However, as our CA measurements showed, the HT of CFs does not lead to significantly improved wettability. Would that effect be enough to explain the improved performance? However, ex situ measured CAs are not representative for operational conditions and therefore can only provide trends for the wetting behavior in application-relevant conditions. It is also worth mentioning here that the investigation of CAs of inhomogeneous and rough surfaces poses experimental difficulties; hence, the CA did vary from one point to another, leading to increased error values.[20] For this reason, it makes sense to limit their evaluation to a qualitative analysis. Moreover, we think it is necessary to provide alternative strategies to determine the wetting behavior of porous felt electrodes.

To overcome this issue an in situ cell was designed to image the wetting behavior and electrolyte invasion and distribution in the electrode using micro-CT measurements. The setup enabled us to investigate the processes taking place in a close-to-application scenario with variable compression rates and pumped electrolytes in a cell hardware of relevant size, where similar cell designs are in use in many other research labs. In-situ X-ray radiography measurements were conducted for all combinations of UT and HT CFs with three different electrolytes (deionized water, 2 M sulfuric acid, and commercial VRFB electrolyte). **Figure 4** shows the different wetting behaviors of GFD 4.6 UT and GFD 4.6 HT 30. The hydrophobic pristine CF reveals a higher threshold against the invasion of water. The water electrolyte invades the electrode material slowly, showing a clear electrolyte boundary with visibly preferred pathways. It must also be mentioned that the electrolyte is forced to pass the CF on the sides of the electrode as a result of the high threshold against its wetting with water. In contrast to these observations, the GFD 4.6 HT 30 sample shows not only a higher wettability but also a different invasion behavior. Even though the material was only slightly more hydrophilic in the CA measurements, here, the water can easily spread in the whole electrode. After the initial contact, on the left side of the electrode, the water fills the CF homogeneously and the electrolyte boundary proceeds quickly to the top and right side of the electrode. This behavior results in a highly flooded electrode after only 29 s, whereas the GFD 4.6 UT electrode was only flooded to a minimal amount after the same time.

The in situ X-ray radiography images were processed further to calculate the theoretical electrolyte filled volume of each electrode. **Figure 5**a shows this evaluation for water. Two different behaviors of the pristine felts could be detected. GFD 4.6 UT is slowly filled with water, as shown in Figure 4, encountering a first threshold after 1 min of operation. The theoretically filled volume increases slowly, from roughly 15% to 20% after 1 h of operation. However, the GFA 6 UT electrode is flooded to a higher ratio after 1 min, encountering also a threshold which is not overcome even after 100 min of operation. The hydrophobic character of the pristine felts can be clearly detected. In contrast to that, all heat-treated samples of the two different felt materials show a significantly improved wetting. All HT samples are flooded to a high theoretical volume of ≈90%, implying only few and small regions of unfilled electrode material. Furthermore, the GFD 4.6 HT felts are slightly more filled than the GFA 6 HT felts. Also, a clear trend is visible—that the HT 30 samples (subjected to HT for a longer time) are filled to a higher degree than the HT 10 samples.

However, tests with water appear less meaningful, as the commercial vanadium electrolyte consists of 2 M sulfuric acid as support for the vanadium species. Therefore, the second choice of the electrolyte was 2 M sulfuric acid to assess the individual influence of the acidic nature of the electrolyte on the wetting behavior. The obtained results are shown in Figure 5b. The pristine CFs reveal an improved wetting with sulfuric acid and are filled to a higher ratio in comparison with the experiments with deionized water. After initial wetting, a first threshold is encountered for both samples; here the GFA 6 UT sample is more filled than the GFD 4.6 UT sample. Both samples filled up slowly with time and reach the same filling degree after 100 min of operation. In contrast to that, the heat-treated samples achieve very

© 2019 The Authors. Published by WILEY-VCH Verlag GmbH & Co. KGaA, Weinheim

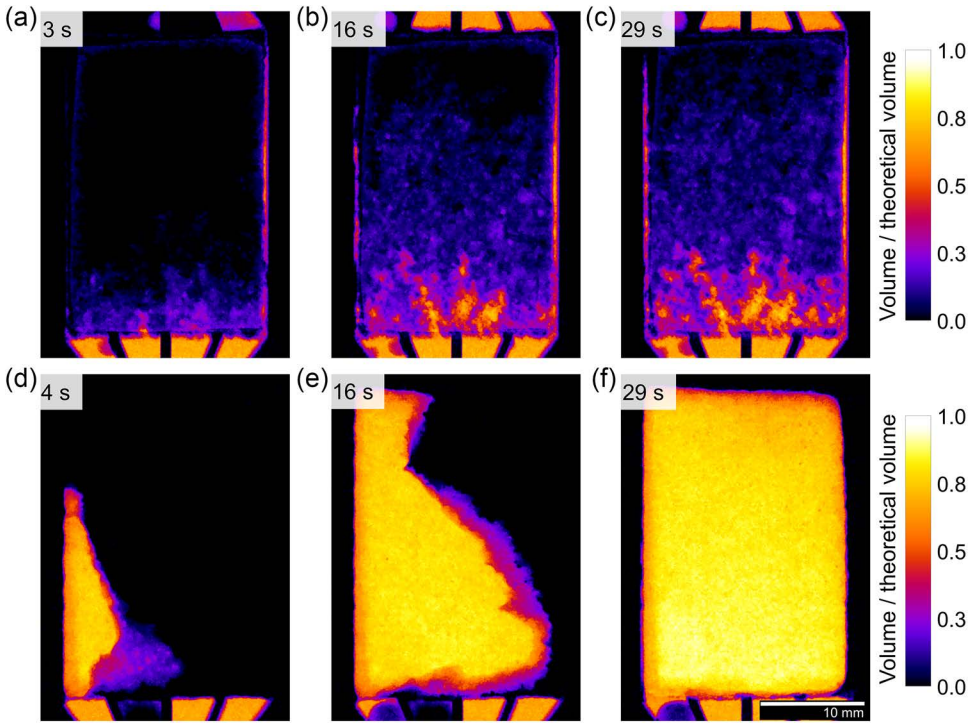

Figure 4. In situ X ray radiography images of the flooding process of a–c) GFD 4.6 UT and d–f) GFD 4.6 HT 30 with deionized water demonstrate the different wetting behaviors of the felt materials, pump rate 5 mL min^{-1}. The electrolyte was pumped through the felts from bottom to top.

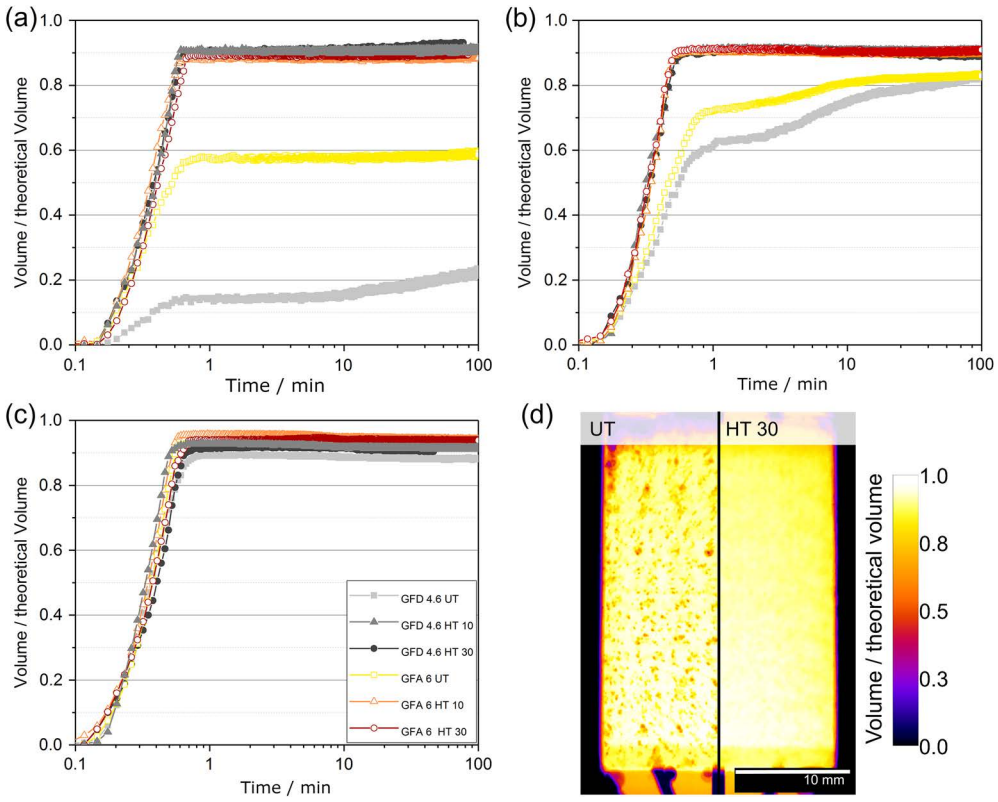

Figure 5. Evaluation of in situ X-ray radiography experiments, calculated theoretical volume, filled with a) deionized water, b) 2 M sulfuric acid, and c) commercial VRFB electrolyte. d) Comparison of differently filled GFD 4.6 electrodes with commercial electrolyte.

© 2019 The Authors. Published by WILEY-VCH Verlag GmbH & Co. KGaA, Weinheim

high filling rates comparable with the experiment conducted with deionized water. After 1 min of operation, all heat-treated electrodes are filled with sulfuric acid to ≈90%. Consequently, the acidic nature of the electrolyte leads to an improved electrolyte invasion for the pristine felts but shows no improvement for the HT samples. It seems that the interactions between the CF and the liquid are stronger in case of sulfuric acid, resulting in comparatively higher filling rates.

Finally, the wetting behavior with commercial vanadium containing the electrolyte was investigated and a surprising phenomenon was observed. All tested electrode materials show nearly no resistance toward wetting with electrolyte. After 30–40 s only, all felt materials are filled to a high and almost the same degree. GFA felts provide minimally higher filling ratios (of around 94%) compared with the GFD felts (around 91%). Additionally, the heat-treated samples of both materials are slightly superior (1–2%) to the untreated felts. Hence, the effect of HT is providing a slightly higher flooding level of the electrode material, but the effect is negligible compared with the one observed with water or sulfuric acid used as the electrolyte. What is even more interesting is the distribution of the electrolyte within the felt. Even though the filling degrees are comparable for all samples with the commercial electrolyte, a difference in the electrolyte distribution can be observed from the radiography images (Figure 5d). The picture shows the overall different distribution of commercial electrolyte in GFD 4.6 UT (left) and GFD 4.6 HT 30 (right). It is shown that the pristine felt shows highly filled domains and small spots with less electrolyte in the electrode.

These less filled areas may only be explained by residual air in the felt electrodes because the material structure is the same for all samples. Even after operation of several hours and high flow rates (10 L h^{-1} not shown here), these unfilled areas did not disappear. This is in strong contrast with the heat-treated felt, which displays homogeneous filling. Additional tomography experiments were conducted for further clarification of this phenomenon. As shown in **Figure 6**a, the dry GFD 4.6 CF consists of a large number of single and thin carbon fibers. However, due to their manufacturing, these carbon fibers tend to form bundles of relatively thick fiber domains in certain parts in the electrode. Electrolyte entering the felt is forced to flow through the felt and is bypassing these denser areas. As a result, these hydrophobic pore/fiber spaces remain nearly unfilled. To confirm this hypothesis, additional tomography experiments were performed with GFD 4.6 UT after 2 h of radiography operation with commercial VRFB electrolyte (see Figure 6b). The tomography slices reveal the 3D nature of the unfilled pore volume. It appears as if these areas form channel-like structures, which are distributed homogeneously. This behavior is in line with the shown cross-sectional slice of the dry felt. These denser areas seem to remain unfilled in the untreated GFD 4.6 felt (dark areas). For a better localization of the unfilled pore volume, a 3D reconstruction was done (see Figure 6c), leading to a better understanding of the wetting behavior of untreated felts and the limitations by the

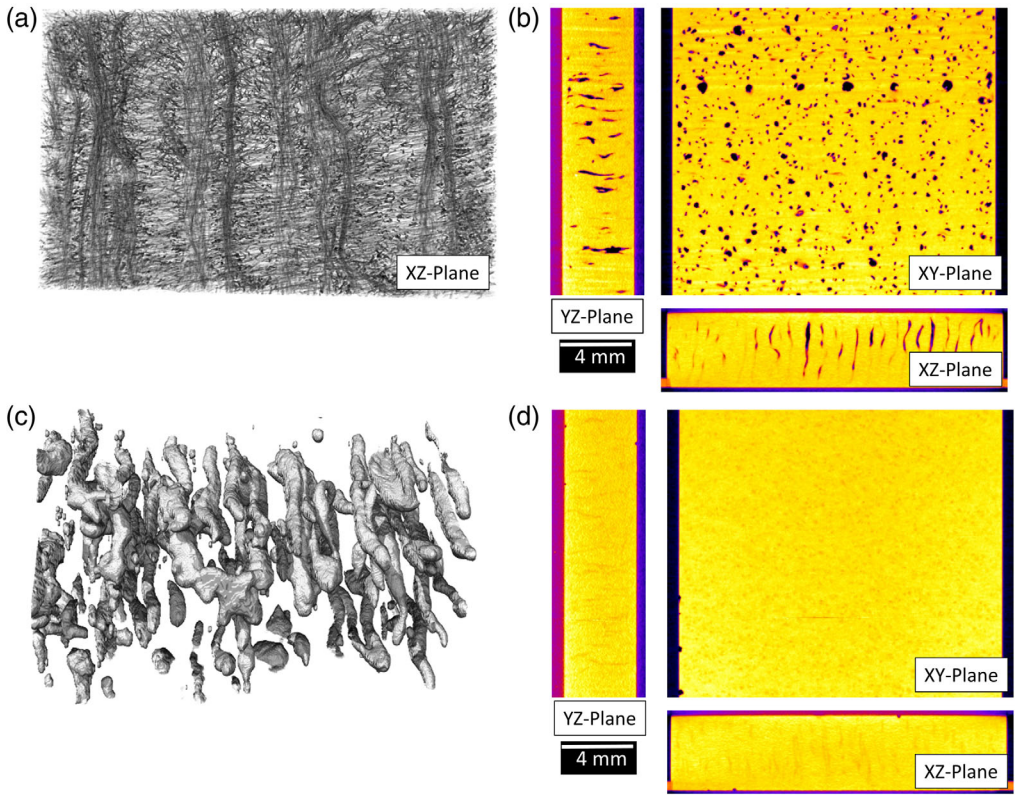

Figure 6. Tomography images a) high-resolved 2D structure of a pristine GFD 4.6 CF. b,d) cross-section images XY, XZ, and YZ planes obtained after 2 h of operation with commercial VRFB electrolyte for GFD 4.6 UT (b) and GFD 4.6 HT 10 (d), and c) unfilled pore volume of a wetted GFD 4.6 UT CF.

© 2019 The Authors. Published by WILEY-VCH Verlag GmbH & Co. KGaA, Weinheim

hydrophobic nature of the material. Obviously, not all fibers in the felt are in contact with electrolyte and the utilization of the felt electrode is limited.

Further tomography experiments were performed with the heat-treated CF (GFD 4.6 HT 10) under equal conditions, to compare both results (see Figure 6d). As the previous radiography experiments revealed, the wetting behavior improved slightly by the HT and led therefore to the additional filling of the denser areas, which—in case of the untreated felt—remain unfilled. But 3D tomography reveals that these domains still exist and can be observed in each cutting plane (Figure 6d), but the contrast is minimized here. Nevertheless, the utilization of the felt electrode should be higher compared with an untreated felt as more fibers seem to be in contact with the electrolyte.

However, our result indicates that thermal HT of CF electrodes does not provide significantly higher filled electrodes but leads to an improved wetting with an increase in the wetted surface. Even though the hydrophilicity was not significantly increased by the thermal treatment for water and sulfuric acid, the achieved theoretical filled volumes with VRFB electrolyte were comparable. The effect of the HT was mainly improving the wetting behavior in areas with a high fiber density, leading to a more homogenously filled electrode. To identify and assess the appropriate influence of a better wetted electrode on the overall performance of a VRFB, more detailed research has to be conducted in the future.

4. Conclusion

CA measurements and in situ X-ray radiography and tomography of pristine and heat-treated commercial CFs were conducted to obtain more insights into the importance of surface wettability as compared with functional groups. An in situ flow cell with a design and size close to those used throughout many research labs was used to monitor the electrolyte invasion and distribution within the porous electrodes. Based on the in situ radiography results with different types of electrolytes, we propose that the enhanced wetting behavior by the thermal treatment of CFs is less important and effective than suggested in earlier publications. Only a negligibly higher pore-filling degree could be observed for all heat-treated samples. A direct, spontaneous, and improved wetting with electrolyte (water and 2 M sulfuric acid) to a very high ratio was observed for all HT samples. For commercial vanadium electrolyte, however, all types of electrodes were flooded in less than 1 min, no matter which pretreatment was applied. Our results necessitate to rethink previously drawn assumptions about the correlation between the improved wetting behavior of the electrodes and the enhanced electrochemical performance of such samples.

Acknowledgements

M.G. and M.S. contributed equally to this work. The authors want to thank the HZB for the allocation of micro-CT measurements time. The provision of commercial CFs by SGL Carbon and VRFB electrolyte by GfE mbH is acknowledged. Likewise, the help of the workshop at Freie Universität Berlin is gratefully appreciated. This work was supported by the Deutsche Forschungsgemeinschaft in the framework of FOR 2397 (grant numbers RO 2454/16-1, KR 3850/6-1, and MA 5039/3-1).

Conflict of Interest

The authors declare no conflict of interest.

Keywords

carbon felts, contact angle measurements, electrolyte wetting, thermal treatments, vanadium redox flow batteries, X-ray radiographies, X-ray tomographies

Received: October 11, 2019
Published online: November 11, 2019

[1] a) J. Noack, N. Roznyatovskaya, T. Herr, P. Fischer, *Angew. Chem., Int. Ed.* **2015**, *54*, 9776; b) M. Skyllas-Kazacos, M. H. Chakrabarti, S. A. Hajimolana, F. S. Mjalli, M. Saleem, *J. Electrochem. Soc.* **2011**, *158*, R55; c) A. Z. Weber, M. M. Mench, J. P. Meyers, P. N. Ross, J. T. Gostick, Q. Liu, *J. Appl. Electrochem.* **2011**, *41*, 1137; d) X. Ke, J. M. Prahl, J. I. D. Alexander, J. S. Wainright, T. A. Zawodzinski, R. F. Savinell, *Chem. Soc. Rev.* **2018**, *47*, 8721.

[2] a) T.-C. Chang, J.-P. Zhang, Y.-K. Fuh, *J. Power Sources* **2014**, *245*, 66; b) L. D. Brown, T. P. Neville, R. Jervis, T. J. Mason, P. R. Shearing, D. J. L. Brett, *J. Energy Storage* **2016**, *8*, 91.

[3] a) M. H. Chakrabarti, N. P. Brandon, S. A. Hajimolana, F. Tariq, V. Yufit, M. A. Hashim, M. A. Hussain, C. T. J. Low, P. V. Aravind, *J. Power Sources* **2014**, *253*, 150; b) K. J. Kim, M.-S. Park, Y.-J. Kim, J. H. Kim, S. X. Dou, M. Skyllas-Kazacos, *J. Mater. Chem. A* **2015**, *3*, 16913; c) T. X. Huong Le, M. Bechelany, M. Cretin, *Carbon* **2017**, *122*, 564.

[4] a) A. Fetyan, G. A. El-Nagar, I. Derr, P. Kubella, H. Dau, C. Roth, *Electrochim. Acta* **2018**, *268*, 59; b) J. Schneider, E. Bulczak, G. A. El-Nagar, M. Gebhard, P. Kubella, M. Schnucklake, A. Fetyan, I. Derr, C. Roth, *Batteries* **2019**, *5*, 16.

[5] a) M. Schnucklake, S. Kuecken, A. Fetyan, J. Schmidt, A. Thomas, C. Roth, *J. Mater. Chem. A* **2017**, *5*, 25193; b) A. Fetyan, J. Schneider, M. Schnucklake, G. A. El-Nagar, R. Banerjee, N. Bevilacqua, R. Zeis, C. Roth, *ChemElectroChem* **2019**, *6*, 130; c) A. Fetyan, I. Derr, M. K. Kayarkatte, J. Langner, D. Bernsmeier, R. Kraehnert, C. Roth, *ChemElectroChem* **2015**, *2*, 2055.

[6] a) B. Sun, M. Skyllas-Kazacos, *Electrochim. Acta* **1992**, *37*, 1253; b) B. Sun, M. Skyllas-Kazacos, *Electrochim. Acta* **1992**, *37*, 2459; c) L. Yue, W. Li, F. Sun, L. Zhao, L. Xing, *Carbon* **2010**, *48*, 3079; d) A. Di Blasi, O. Di Blasi, N. Briguglio, A. S. Aricò, D. Sebastián, M. J. Lázaro, G. Monforte, V. Antonucci, *J. Power Sources* **2013**, *227*, 15.

[7] a) P. Han, H. Wang, Z. Liu, X. Chen, W. Ma, J. Yao, Y. Zhu, G. Cui, *Carbon* **2011**, *49*, 693; b) L. Eifert, R. Banerjee, Z. Jusys, R. Zeis, *J. Electrochem. Soc.* **2018**, *165*, A2577.

[8] W. Li, J. Liu, C. Yan, *Electrochim. Acta* **2011**, *56*, 5290.

[9] a) D. Schröder, C. L. Bender, T. Arlt, M. Osenberg, A. Hilger, S. Risse, M. Ballauff, I. Manke, J. Janek, *J. Phys. D: Appl. Phys.* **2016**, *49*, 404001; b) R. Banerjee, N. Ge, C. Han, J. Lee, M. G. George, H. Liu, D. Muirhead, P. Shrestha, A. Bazylak, *Int. J. Hydrogen Energy* **2018**, *43*, 9757; c) N. Bevilacqua, M. G. George, S. Galbiati, A. Bazylak, R. Zeis, *Electrochim. Acta* **2017**, *257*, 89.

© 2019 The Authors. Published by WILEY-VCH Verlag GmbH & Co. KGaA, Weinheim

[10] a) S. Alrwashdeh, H. Markötter, J. Haußmann, J. Scholta, A. Hilger, I. Manke, **2016**, *72*, 99; b) S. S. Alrwashdeh, H. Markötter, J. Haußmann, T. Arlt, M. Klages, J. Scholta, J. Banhart, I. Manke, *Energy* **2016**, *102*, 161; c) R. Banerjee, N. Ge, J. Lee, M. G. George, S. Chevalier, H. Liu, P. Shrestha, D. Muirhead, A. Bazylak, *J. Electrochem. Soc.* **2017**, *164*, F154.
[11] F. Tariq, J. Rubio-Garcia, V. Yufit, A. Bertei, B. K. Chakrabarti, A. Kucernak, N. Brandon, *Sustainable Energy Fuels* **2018**, *2*, 2068.
[12] R. Banerjee, N. Bevilacqua, L. Eifert, R. Zeis, *J. Energy Storage* **2019**, *21*, 163.
[13] K. V. Greco, A. Forner-Cuenca, A. Mularczyk, J. Eller, F. R. Brushett, *ACS Appl. Mater. Interfaces* **2018**, *10*, 44430.
[14] N. Bevilacqua, L. Eifert, R. Banerjee, K. Köble, T. Faragó, M. Zuber, A. Bazylak, R. Zeis, *J. Power Sources* **2019**, *439*, 227071.
[15] K. Heiland, D. J. T. Hill, J. H. O'Donnell, P. J. Pomery, *Polym. Adv. Technol.* **1994**, *5*, 116.
[16] J. Schindelin, I. Arganda-Carreras, E. Frise, V. Kaynig, M. Longair, T. Pietzsch, S. Preibisch, C. Rueden, S. Saalfeld, B. Schmid, J.-Y. Tinevez, D. J. White, V. Hartenstein, K. Eliceiri, P. Tomancak, A. Cardona, *Nat. Methods* **2012**, *9*, 676.
[17] a) D. M. Kabtamu, J.-Y. Chen, Y.-C. Chang, C.-H. Wang, *J. Power Sources* **2017**, *341*, 270; b) L. Dai, Y. Jiang, W. Meng, H. Zhou, L. Wang, Z. He, *Appl. Surf. Sci.* **2017**, *401*, 106.
[18] H. Fink, J. Friedl, U. Stimming, *J. Phys. Chem. C* **2016**, *120*, 15893.
[19] S. Zhong, C. Padeste, M. Kazacos, M. Skyllas-Kazacos, *J. Power Sources* **1993**, *45*, 29.
[20] A. Marmur, *Soft Matter* **2006**, *2*, 12.

© 2019 The Authors. Published by WILEY-VCH Verlag GmbH & Co. KGaA, Weinheim